CELLULAR REPROGRAMMING
Volume 12, Number 4, 2010

DOI: 10.1089/cell.2009.0079

Expansion and Characterization of Human Embryonic Stem Cell-Derived Osteoblast-Like Cells

Premjit Arpornmaeklong, Zhuo Wang, Michael J. Pressler, Shelley E. Brown, and Paul H. Krebsbach

Abstract

Human embryonic stem cells (hESCs) have the potential to serve as a repository of cells for the replacement of damaged or diseased tissues and organs. However, to use hESCs in clinically relevant scenarios, a large number of cells are likely to be required. The aim of this study was to demonstrate an alternative cell culture method to increase the quantity of osteoblast-like cells directly derived from hESCs (hESCs-OS). Undifferentiated hESCs were directly cultivated and serially passaged in osteogenic medium (hESC-OS), and exhibited similar expression patterns of osteoblast-related genes to osteoblast-like cells derived from mesenchymal stem cells derived from hESCs (hESCs-MSCs-OS) and human bone marrow stromal cells (hBMSCs-OS). In comparison to hESCs-MSCs-OS, the hESCs-OS required a shorter expansion time to generate a homogenous population of osteoblast-like cells that did not contain contaminating undifferentiated hESCs. Identification of human specific nuclear antigen (HuNu) in the newly formed bone in calvarial defects verified the role of the transplanted hESCs-OS as active bone forming cells *in vivo*. Taken together, this study suggests that osteoblast-like cells directly derived from hESCs have the potential to serve as an alternative source of osteoprogenitors for bone tissue engineering strategies.

Introduction

Recent reports and preclinical studies have demonstrated that cell-based bone tissue engineering strategies may be capable of promoting functional reconstruction of skeletal defects by transplanting adequate numbers of competent osteoprogenitor cells on biomaterial scaffolds. Cell–scaffold constructs seeded with osteoprogenitor cells directly participate in bone regeneration and respond to external and local biological stimuli (Cancedda et al., 2003; Krebsbach et al., 1998; Kwan et al., 2008). To facilitate clinical application of cell-based therapy, it is necessary to develop reproducible differentiation protocols that generate osteoprogenitor cells with consistent bone formation capacity on a large scale (Bianco and Robey, 2001; Martin et al., 1997).

With the ability to form bone in skeletal defects and the ease of harvesting, human bone marrow stromal cells (hBMSCs) may become a reliable source of multipotent stem cells for bone cell transplantation (Derubeis and Cancedda, 2004). However, donor site morbidity and limited amounts of tissue prevent hBMSCs from being an ideal source of cells for cell-based bone tissue engineering (Kwan et al., 2008; Lannert et al., 2008). Similar to hBMSCs, adipose tissue represents an alternative source of adult stem cells (Bunnell et al., 2008). However, the numbers of adult stem cells are limited, decrease with age (De Ugarte et al., 2003; Pittenger et al., 1999) and are present at different stages of differentiation at the time of harvest (Quarto et al., 1995).

Human embryonic stem cells (ESCs) may have the potential to serve as a source of bone forming cells based on their pluripotency and unlimited self-renewal capacity, and because they can be directed to differentiate into specific lineages such as osteoblasts (Heng et al., 2004; Kwan et al., 2008). Potential advantages of hESCs over cell sources such as BMSCs and other adult stem cells for regenerating bone *in vivo* are their unlimited growth and differentiation potential, accessibility, and a lack of donor site morbidity (Carpenter et al., 2003; Fenno et al., 2008).

Osteoblast-like cells can be derived through osteogenic induction of hESCs-derived mesenchymal stem cells (hESCs-MSCs) (Arpornmaeklong et al., 2009; Barberi et al., 2005; Brown et al., 2009; Olivier et al., 2006; Trivedi and Hematti, 2007), through direct osteogenic differentiation of embryoid bodies (EBs) in osteogenic medium (Bielby et al., 2004; Cao et al., 2005; Sottile et al., 2003) or after coculture of EBs with primary bone cells (Ahn et al., 2006). The differentiation of

Department of Biologic and Materials Sciences, University of Michigan School of Dentistry, Ann Arbor, Michigan

osteoblast-like cells from hESCs may also be achieved by omission of the EB stage, in which progression of osteogenic differentiation of hESCs has been reported for a continuous culture period of 25 days after induction (Karner et al., 2007, 2009; Karp et al., 2006). Previous studies demonstrated that hESCs at the EB stage are capable of responding to different osteogenic stimuli and differentiating into osteoblast-like cells with the ability to form bone (Kim et al., 2008; Tremoleda et al., 2008). In the subcutaneous implantation method, osteoblast differentiation was induced by coculturing EB stage cells with primary osteoblasts for 14 days prior to transplantation (Kim et al., 2008). This contrasts with diffusion chamber studies in which EBs and hESC aggregates were exposed to osteogenic medium for 4 days prior to transplantation (Tremoleda et al., 2008). Despite these studies, further development is required to generate large numbers of an enriched osteoblast-like cell population with no contamination of pluripotent cells and other cell types.

Contamination of hESC-derived cultures with different cell types and the persistence of undifferentiated cells in the culture system raises concerns about the applicability of these cells for therapeutic use in humans (Karner et al., 2007, 2009). Additionally, it is possible that the numbers of osteogenic cells derived from continuous cell cultures could be a limiting factor. Therefore, a method that involves the direct induction and restriction of hESCs into cells of the osteoblastic lineage and the stable expansion of large numbers of hESCs differentiated toward an osteoblast phenotype may enable the application of differentiated hESCs in bone regeneration.

The goal of this study was to demonstrate an alternative cell culture method to generate large numbers of osteoblast-like cells by expanding hESC-derived osteoblast-like cells in osteogenic medium (hESCs-OS) and to compare the differentiation pattern of hESCs-OS to hESCs-MSC-derived osteoblast-like cells (hESCs-MSCs-OS). The strategy was to directly induce osteoblastic differentiation of hESCs in osteogenic medium by omitting the EB stage. Instead, hESCs dissociated into single cells were directly incubated in osteogenic medium and expanded as hESC-derived osteoblast-like cells through serial passaging in osteogenic medium. Subsequently, osteoblastic differentiation patterns of the expanded hESCs-OS were characterized in two- and three-dimensional cell culture systems and compared to hESCs-MSCs-OS and hBMSC-derived osteoblasts (hBMSCs-OS). To verify functional differentiation and osteoblastic phenotype stability, the bone regeneration capacity of these cells was investigated in a calvarial defect model.

Materials and Methods

Human embryonic stem cell culture

Human embryonic stem cells (hESCs) (BG01, Bresagen, Inc., Atlanta, GA, USA) were cultivated on irradiated mouse embryonic fibroblast (MEF) feeder layers following the established protocol of the University of Michigan Stem Cell Core. Human ESCs were maintained in serum-free growth medium comprised of 80% DMEM-F12 supplemented with 20% (v/v) knockout serum replacement (KOSR), 200mM L-glutamine, 10mM nonessential amino acids (all from Gibco/Invitrogen, Carlsbard, CA, USA), 14.3M β-mercaptoethanol (Sigma, St. Louis, MO, USA), and 4ng/mL bFGF (Invitrogen). Cell cultures were incubated at 37°C in 5% CO_2 at 95% humidity and manually passaged every 7 days. Culture medium was changed every day.

Induction of osteogenic differentiation of hESCs

To induce osteoblast differentiation without going through the EB stage, undifferentiated hESCs were harvested in TrypLE^{TM} Select (Gibco) at 37°C for 3 min and dissociated into a suspension of single cells. Cells were then transferred to osteogenic medium and seeded on fibronectin-coated plates (BD Biosciences, San Jose, CA, USA) at a ratio of 1:1.

Osteogenic medium was comprised of 90% α-MEM (Gibco), 10% heat-inactivated fetal bovine serum (FBS) (Gibco), 50μM ascorbic acid, 10mM β-glycerophosphate, and 100 nM dexamethasone (all from Sigma) (Sottile et al., 2003). Culture medium was changed three times a week. The differentiated cells (hESCs-OS) were maintained in primary passage (P0) for 14 days. Subsequently, confluent cells were dissociated with trypsin and ethylenediaminetetraacetic acid (0.25% Trypsin/EDTA) (Gibco). The dissociated cells were seeded at a ratio of 1:2 in the first passage (P1) and regularly passaged at confluence on days 5–6 at a ratio of 1:3 in the subsequent passages on tissue culture plates. A karyotype analysis was performed by cytogenetic analysis on 20-G banded metaphase cells of hESCs-OS at passages 5 and 10 (Cell Line Genetics, Madison, WI, USA). All investigations reported here were performed on differentiated cells at passage 5 unless stated otherwise.

Induction of osteogenic differentiation of hESC-derived mesenchymal stem cells (hESCs-MSCs)

Human ESCs were induced to differentiate into mesenchymal stem cells (hESCs-MSCs) and characterized for expression of MSC phenotypes as described previously (Arpornmaeklong et al., 2009). In brief, aggregates of undifferentiated hESCs were cultured in mesenchymal stem cell culture medium (MSC medium) consisting of 10% heat inactivated fetal bovine serum (Gibco) and were then regularly passaged at confluence (7–10 days) at a ratio of 1:3. Differentiated cells derived from these culture conditions at passages 6–7 were designated hESCs-MSCs and used in the analysis for mesenchymal stem cell (MSC) phenotypic characterization and induction of osteogenic differentiation.

To induce osteogenic differentiation, hESCs-MSCs were cultured in osteogenic medium and passaged regularly at 80% confluence. The differentiated cells passaged in osteogenic medium for the fourth time (hESCs-MSCs-OS) were used in the analyses.

Induction of osteogenic differentiation of human bone marrow stromal cells

Human bone marrow was collected from patients undergoing iliac bone graft procedures with University of Michigan institutional review borad approval. Bone marrow stromal cells (BMSCs) were isolated as previously described (Krebsbach et al., 1997). Human BMSCs at passage 4 were subjected to osteogenic differentiation in osteogenic medium and regularly passaged at 80% confluence at a ratio of 1:3. Human BMSCs expanded in osteogenic medium for the

fourth time (hBMSCs-OS) served as a positive control in the study.

Three-dimensional cell culture

For three-dimensional cell cultures, 5×3 mm 3D collagen composite scaffolds (BD Biosciences Discovery Labware, Bedford, MA, USA) were neutralized in DMEM-F12 culture medium (Gibco) supplemented with 10% FBS overnight at 37°C. Prior to cell seeding, excess fluid was removed from the scaffolds using filter paper. Hydrated scaffolds were placed in 60-mm bacterial cell culture plates (BD Falcon, Bedford, MA, USA).

Differentiated hESCs in osteogenic medium at passage 9 and 80% confluence were trypsinized and 1×10^5 differentiated cells were suspended in 30 μL of 20 mg/mL human fibrinogen (Sigma) in a 1.5-mL tube. Subsequently, 5 μL of human thrombin (100 unit/mL) (Sigma) was added to the fibrinogen-cell suspension, thoroughly mixed, and consequently seeded on the collagen scaffolds. Cell seeded scaffolds were incubated in a six-well cell culture plate with 0.5 mL culture medium/well in a humidified incubator at 37°C with 5% CO_2 for 2 h, and then 10 mL of osteogenic medium was added to each plate. The cell constructs were cultured in osteogenic medium for 21 days and culture medium was replaced every 3 days (Arpornmaeklong et al., 2009). Alkaline phosphatase, collagen type I, osteonectin, osteocalcin, and mineralization of the extracellular matrix were examined using immunohistochemical evaluation and von Kossa staining, respectively ($n=3$).

Flow cytometrical analysis of cell surface antigens

The hESCs differentiated in osteogenic medium (hESCs-OS) at passages 5 and 9 were harvested using 0.25% collagenase in DPBS (Gibco) and 0.25% Trypsin/EDTA (Gibco). After neutralization, single cell suspensions were washed in cold bovine serum albumin (BSA, 0.5% w:v) (Sigma) in DPBS and incubated at a concentration of 1×10^6 cells/mL in 1 μg/mL unconjugated goat antihuman IgG (Caltag/Invitrogen) on ice for 15 min to block nonspecific binding. Samples (2.5×10^5 cells) were then incubated on ice with the optimal dilution of conjugated monoclonal antibody (mAb) in 1 μg/mL unconjugated goat antihuman IgG in the dark. All mAbs were of the immunoglobulin G1 (IgG1) isotype. The following conjugated antibodies were used in the analysis: Allophycocyanin (APC)-conjugated monoclonal antibodies (mAbs) against CD44 (BD Pharmingen™, San Jose, CA, USA) and Alkaline Phosphatase (R&D Systems, Minneapolis, MN, USA); Fluorescein istothiocyanate (FITC)-conjugated mAb againsts CD45 (all from BD); Phycoerythrin (PE)-conjugated mAbs against CD49a and CD73 (all from BD), CD105 (eBioscience, San Diego, CA, USA) and STRO-1 (Santa Cruz Biotechnology, Santa Cruz, CA, USA); and Phycoerythrin-Cy5 (PE-Cy5)-conjugated mAb againsts CD34 (BD). After 30 min incubation, cells were washed twice in cold 0.5% BSA in DPBS. Double staining of APC-ALP and PE-STRO-1 was performed to analyze coexpression of the antigens. Nonspecific fluorescence was determined by incubating cells with conjugated mAbs raised against anti-human IgG1 (all from BD).

At least 10,000 events were acquired for each sample using a fluorescent-activated cell-sorting instrument (FACSCalibur, Becton Dickinson, San Jose, CA, USA). Cell flow cytometry data were analyzed using CELLQUEST software (Becton Dickinson). Analyses on hESCs-OS at passage 5 for MSC surface markers and at passage 9 for ALP and STRO-1 double staining were performed on four and two separate cell strains, respectively.

Characterization of osteoblastic phenotypes

A leukocyte alkaline phosphatase kit (Sigma-Aldrich Chemie GmbH, Steinheim, Germany) was used for alkaline phosphatase (ALP) staining following the recommended protocol. For von Kossa staining of mineralized matrix on cell culture plates and on the collagen scaffolds, cells were fixed in Z-FIX aqueous buffered zinc formalin (Anatech LTD, Battle Creek, MI, USA) for 4min and histological sections were deparaffinized and immersed in 5% silver nitrate (Sigma), followed by fixation in 5% sodium thiosulfate (Sigma) and counterstaining with a 5% nuclear fast red solution as described (Arpornmaeklong et al., 2009). Alkaline phosphatase and von Kossa stainings were performed on hESCs-OS at passage 5 on culture days 14 and 21, respectively.

Alkaline phosphatase activity was measured for hESCs-OS, hESCs-MSCs-OS, and hBMSCs-OS on days 3, 7, 14, and 21 and osteocalcin secretion was measured on days 7, 14, and 21. To collect the samples for measuring protein content, ALP activity, and osteocalcin secretion, cells were washed with DPBS (without calcium and magnesium, Gibco) and incubated with serum free medium overnight. Subsequently, the medium was collected and stored at −70°C prior to the Gla-Type Osteocalcin enzyme immunoassay (EIA) for quantitative determination of human Gla-OC in culture supernatants. Further, the cells were washed with DPBS and stored at −20°C prior to the ALP and protein analyses (Arpornmaeklong et al., 2009).

The protein concentration was measured on the same samples for the ALP activity and osteocalcin assays. The concentration of protein from cell lysates was determined according to the manufacturer's instructions (Biorad Protein assay kit, Bio-Rad, Hercules, CA, USA). Quantification of osteocalcin in the serum free cell culture medium was performed according to the manufacturer's instruction using the Gla-type Osteocalcin EIA kit (Takara, Shiga, Japan). Alkaline phosphatase and osteocalcin levels were normalized by the protein concentration of the sample. A total of five samples from each group from three independent experiments were tested at each time point (Arpornmaeklong et al., 2009).

Immunohistochemical staining

To identify deposition of bone matrix on collagen scaffolds, mouse monoclonal antibody (mAb) raised against ALP diluted at a ratio of 1:100 and rabbit mAb raised against osteonectin (Anti-SPRAC) diluted at a ratio of 1:200 (all from Sigma Life Science, St. Louis, MO, USA), mouse mAb raised against collagen type I diluted at a ratio of 1:200, and mouse mAb raised against osteocalcin diluted at a ratio of 1:100 (all from Abcam, Cambridge, MA, USA) were applied.

To identify the origin of transplanted cells, paraffin embedded sections were stained with mouse mAb raised against human specific nuclear antigen (HuNu) diluted at a ratio of 1:50 (Chemicon International/Millipore, Billerica,

CA, USA). Negative controls were obtained by omitting the primary monoclonal antibody. Throughout the study, the R.T.U. Vectastain Universal Elite ABC Kit and the Vector AEC, DAB, and NovaRed (Red) peroxidase substrate kits (Vector Laboratories, Burlingame, CA, USA) were used. Immunohistochemical staining was performed according to the manufacturer's instructions. Gill's formula Hematoxylin (Vector Laboratories) was used for counterstaining. Histological slides were covered with Crystal Mount Aqueous Mounting Medium (Sigma) and analyzed by light microscopy (Nikon Eclipse E600, Nikon, Shinakawa-ku, Japan).

Quantitative real-time reverse-transcriptase polymerase chain reaction (qRT-PCR)

Quantitative RT-PCR was performed to determine expression levels of pluripotency regulator genes, markers of cells representative of three germ layers, and osteoblast-associated genes. Gene expression levels were determined for hESCs, hESCs in growth medium, hESCs-OS at primary, fifth, and ninth passages, hESCs-MSCs-OS, and hBMSCs-OS. Total RNA was extracted using Trizol (Invitrogen) and 1μg of RNA was reverse transcribed into cDNA using Superscript III Reverse Transcriptase (Invitrogen). Two microliters of the diluted reverse transcribed cDNA (RT reaction, 1:5 in RNase free-water) was amplified in a 30μL PCR assay volume, using the TaqMan Gene Expression Master Mix (Applied Biosystems, Foster City, CA, USA) and 20×Target primers and Probe (unlabled PCR primers and a FAM™ dye-labled TaqMan® minor groove binder (MGB) probe) (Applied Biosystems). Genes and primers used are listed in Table 1. The expression of the genes was measured by qRT-PCR on an ABI Prism 7700 Sequence Detection System (Applied Biosystems). The levels of the target genes were correlated to standard concentrations and normalized to the levels of beta-actin (ACTB) as an endogenous reference. Subsequently, the expression levels of investigated genes were normalized to the expression levels of undifferentiated hESCs (BGO1, passage 58) and reported as fold changes.

Preparation of cell constructs for transplantation

The hESCs differentiated in osteogenic medium (hESCs-OS) at passages 5 and 10 were harvested using 0.25% collagenase (Gibco) in DPBS and 0.25% trypsin–0.53mM EDTA (Gibco). To prepare the cell constructs for transplantation, cell pellets were resuspended in 40mg/mL human plasma fibrinogen at 3×10^6 cells per 40μL in 1.5-mL tubes and absorbed to a 5×3 mm gelatin sponge (Pharmacia & Upjohn Co., Kalamazoo, MI). Ten microliters of human plasma thrombin (100 Unit/mL) (Sigma) was applied on the sponge to initiate fibrin clotting.

Surgical procedure and cell transplantation in craniofacial defect model

All procedures were approved by the University of Michigan Committee on the Use and Care of Animals. Twenty-two 5-week-old female immunocompromised mice (N:NIH-bg-nu-xid; Harlan Sprague Dawley, Research Triangle park, NC, USA) (9 mice for hESCs-OS at passage 5, 10 mice for hESCs-OS at passage 10, and 3 mice for control defects without cells) were anesthetized with intraperitoneal injections of ketamine (Ketaset, 75mg/kg, Fort Dodge Animal Health, Fort Dodge, IA, USA) and xylazine (Ansed, 10mg/kg, Lloyd laboratories, Bedford, OH, USA). A semilunar scalp incision was made from right to left of the post-auricular areas, and a full-thickness flap was elevated. The periosteum overlying the calvarial bone was completely resected. A trephine was used to create a 5-mm craniotomy defect centered on the sagittal suture and the calvarial disk was removed. Subsequently, cell constructs were transplanted into the defect sites. The incisions were closed with 4-0 Chromic Gut suture (Ethicon/Johonson&Jhonson, Somerville, NJ, USA) (Krebsbach et al., 1997). All mice were sacrificed 5–6 weeks after the implantation.

Microcomputed tomography analysis

Individual calvaria were immediately fixed in aqueous buffered zinc formalin (Z Fix, Anatech, MI, USA) for 24h and subsequently stored in 70% alcohol (Histoprep, Fisher Scientific, IL, USA) to the time of micro computed tomography (μCT) and histological analyses.

For μCT analysis, nine calvarial samples and three control calvariae in water were scanned by μCT (eXplore Locus SP, GE Healthcare Pre-Clinical Imaging, London, Ontario, Canada). Measurements were taken at an operating voltage of 80kV and 80 mA of current, with an exposure time of 1600 msec using the Parker method scan technique, which rotates the sample 180 degrees plus a fan angle of 20 degrees. The effective voxel size of the reconstructed image was 18μm^3. Houndsfield unit calibration was performed with a phantom containing water, air, and a cortical bone mimic.

Table 1. List of Primers Used in the qRT-PCR Analysis

Names/symbols	*Gene description*	*Catalog numbers*
Alpha-fetoprotein (AFP)	Alpha-fetoprotein	Hs00173490_m1
Beta-actin (ACTB)	Human ACTB (actin, beta) endogenous control	4333762T
Beta III tubulin (TUBB3)	Tubulin, Beta III	Hs00964962_g1
Bone sialoprotein (IBSP)	Integrin-binding sialoprotein	Hs00173720_m1
Brachyury (T)	Brachyury homolog (mouse)	Hs00610080_m1
Collagen type I (COL 1A1)	Collagen, type I, alpha 1Type I collagen	Hs00164004_m1
Nanog	Nanog homeobox	Hs02387400_g1
Oct3/4 (POU5F1)	POU class 5 homeobox 1	Hs03005111_g1
Osteocalcin (BGLAP)	Bone gamma-carboxyglutamate (gla) protein	Hs01587814_g1
Runx2	Runt-related transcription factor 2	Hs00231692_m1
Sox2	SRY (sex determining region Y)-box	Hs01053049_s1

Reconstructed images were analyzed with Microview v2.1.0 software (GE Healthcare Pre-Clinical Imaging, London, Ontario, Canada). A threshold value of 1000 was used to obtain the 3D images. A cylindrical region of interest (ROI) of 5×1.3 mm was centered over the defect site. Total volume of bone within the ROI was measured. Bone mineral density (BMD, mg HA/ccm) was calculated and determined with an internal reference in Houndsfield units. The BMD was then normalized to the control as previously described (Hu et al., 2007).

Histological assessment

For histological analysis, calvariae were decalcified with a 10% EDTA solution for 2 weeks, dehydrated with a gradient of alcohols and embedded in paraffin. Coronal sections of 5 μm in thickness were cut and stained with hematoxylin and esosin (following standard procedures of the University of Michigan School of Dentistry, Histology Core). Subsequently, the sections were reacted with a monoclonal antibody against human specific nuclear antigen (HuNu) as stated in the immunohistochemical section. The histological sections were visualized with an inverted microscope Eclipse TE300 (Nikon, Melville, NY, USA) to examine the newly formed bone and hematopoietic bone marrow formation in these critical size calvarial defects (Arpornmaeklong et al., 2009; Hu et al., 2007).

Statistical analysis

Data were expressed as the mean value±the standard error of the mean (mean±SEM) and analyzed by one-way analysis of variance. The levels of statistical significance were set at $p< 0.05$.

Results

Dissociated hESCs directly responded to osteogenic medium and differentiated into osteoblast-like cells

At the initiation of osteogenic induction, the dissociated hESCs in osteogenic medium (hESCs-OS) expressed osteoblast-associated genes, pluripotent regulator genes, and markers consistent with differentiation into different lineages (Fig. 1). During the 14 day culture period, the expression of osteoblast-associated genes (runx2, Col 1A1, and osteonectin) from the hESCs-OS at the primary passage significantly increased from day 3 to day 14 ($p< 0.05$) and were significantly higher than the levels measured from hESCs in culture medium without osteogenic supplementation (Fig. 1A–C). In contrast, expression levels of the pluripotent regulator gene, oct3/4, decreased from day 3 to day 14, and on day 14 expression was significantly lower than cell cultures in culture medium without osteogenic supplementation ($p <0.05$) (Fig. 1D). These findings indicated a response of the hESCs to the osteogenic stimuli.

Serial passaging in osteogenic medium directed and restricted differentiation of dissociated hESCs into the osteoblastic lineage.

The presence of pluripotency markers, oct3/4, nanog, and sox2, as well as markers of endodermal (alpha-fetoprotein, AFP), mesodermal (brachyury, T), and ectodermal (beta III tubulin, BTUB) lineages in hECSs in osteogenic medium in

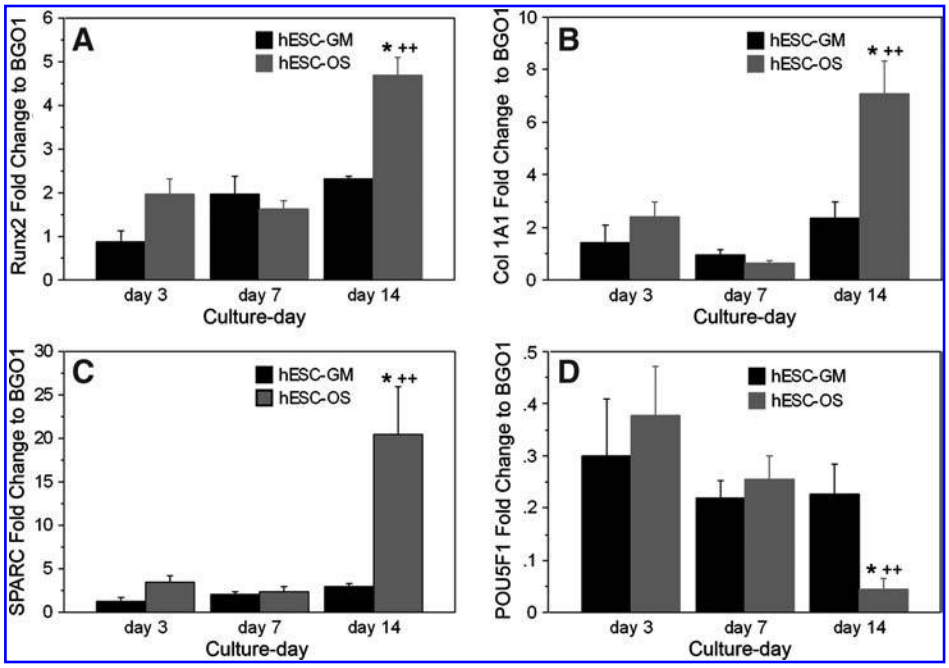

FIG. 1. Expression profiles of osteoblast-associated genes and pluripotent regulator genes from hESCs in growth (hESC-GM) and osteogenic supplement (hESC-OS) medium. (**A**) Runx2, (**B**) Collagen type I (Col 1A1), (**C**) Osteonectin (SPARC), and (**D**) Oct3/4 (POU5F1). Results are presented as the mean ± SEM of three independent experiments normalized to the expression level of undifferentiated hESCs (BGO1). The symbol (*) represents significantly different expression levels relative to the other groups at the same time point ($p < 0.05$) and (++) represents significantly higher expression levels when compared to the levels in the same group at different time points ($p < 0.01$).

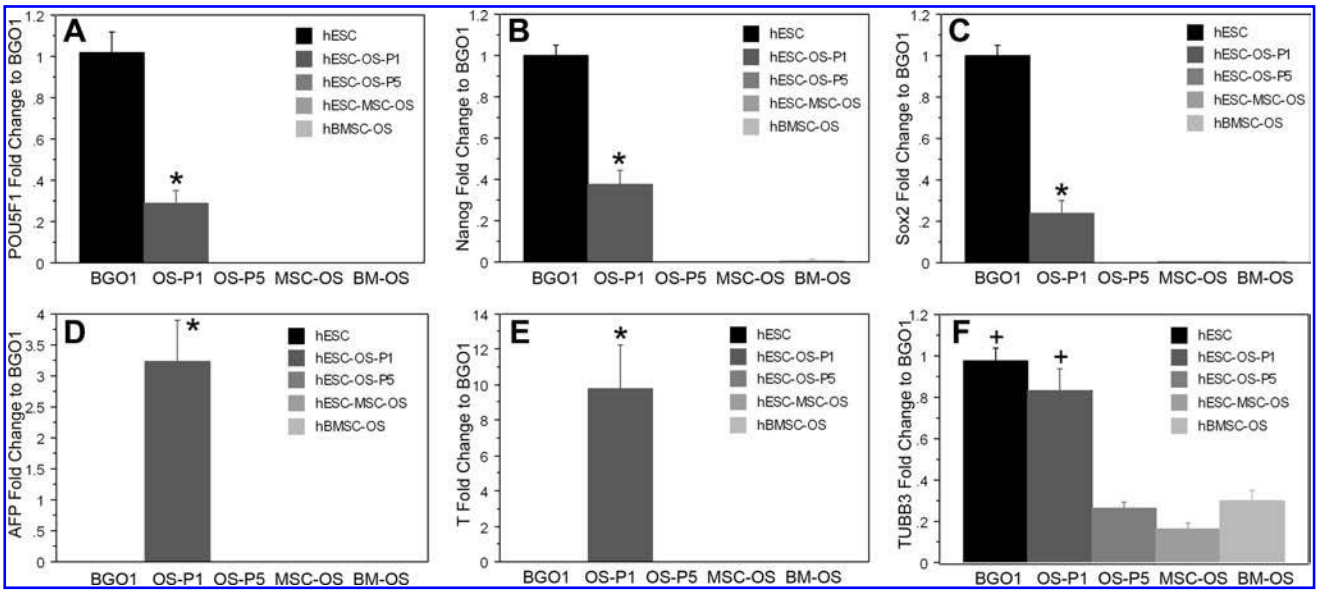

FIG. 2. Quantitative PCR analysis of hESCs and derivative cells. (**A**) oct3/4 (POU5F1), (**B**) nanog, (**C**) sox2, (**D**) alpha-fetoprotein (AFP), (**E**) T-brachyury (T), and (F) β-III tubulin (TUBB3). The expression of these genes in undifferentiated hESCs (hESC, BGO1) and hBMSCs in osteogenic medium (hBMSC-OS, BM-OS) was assessed as positive and negative controls, respectively. Results are presented as the mean ± SEM of three independent experiments normalized to the expression levels of the undifferentiated hESCs (BGO1). The symbol (*) represents significantly different levels relative to the expression of other groups ($p < 0.01$). In **F** (+) represents both groups (BGO1 and OS-P1) as having a significantly higher expression relative to the expression of other groups ($p < 0.01$).

the primary passage indicated that at an early stage of osteogenic induction, differentiation of hESCs was not restricted to the osteoblastic lineage. Instead, hESCs differentiated into various cell types, including osteoblast-like cells (Figs. 1 and 2). However, when hESCs-OS, hESCs-MSCs-OS, or hBMSCs-OS were cultured for 5 passages, the cells failed to express oct3/4, nanog, sox2, AFP, and brachyury, and were similar to the expression levels in hBMSCs-OS (Fig. 2A–E). Low levels of beta-III tubulin were expressed in all three cultures during this culture period (Fig. 2F). Taken together, these findings suggest that serial passaging in osteogenic medium directed and restricted the differentiation of hESCs into cells of the osteoblastic lineage (Figs. 1 and 2).

Human ESCs-OS at higher passages exhibited homogenous cell morphology and phenotypes of osteoblast-like cells, suggesting the restriction of differentiation over time (Fig. 3A–D). The cultures consisted of spindle shaped cells that exhibited ALP activity and developed a mineralized extracellular matrix (ECM) (Fig. 3B–D). Cell surface markers consistent with MSCs and osteoprogenitor cells were also evaluated. The average expression levels of surface antigens in hESCs-OS and hESCs-MSCs-OS were CD44 (99.40±0.08%), CD73 (99.25±0.19%), ALP (42.22±6.5%), and ALP coexpressing CD105 (36.61± 4.23%) (Fig. 4). Significant differences in the expression levels between hESCs-OS and hESCs-MSCs-OS were observed for CD49a and CD105. The levels of CD49a and CD105 in hESCs-MSCs-OS were significantly higher than hESCs-OS (CD49a: 80.73±5.98 vs. 53.31±11.1, $p< 0.05$ and CD105: 96.85±2.5 vs. 80.72±1.98, $p< 0.01$, respectively). The analysis revealed that 89 and 83% of the ALP expressing cells from hESCs-OS and hESCs-MSCs-OS, respectively, coexpressed CD105 (37.7± 3.8% in hESCs-OS and 35.5±8.5% in hESCs-MSCs-OS) (Fig. 4). Expression of the hematopoietic markers, CD34 and CD45 was not found (<0.1% of positive cells) (data not show).

The numbers of cells expressing ALP and STRO-1, a MSC surface marker, from hESCs-OS were further examined in hESCs-OS at passage 9. Side-scatter analysis demonstrated that ALP expressing cells from hESCs-OS at passage 9 represented 53% of the total cells. The numbers of cells that doubly expressed ALP and STRO-1 were 4%, and only 1% of total cells expressed STRO-1 only (Fig. 5).

Expanded hESC-derived osteoblast-like cells demonstrated comparable osteoblastic differentiation patterns to hESCs-MSCs-OS and hBMSCs-OS

During a 21-day culture period, hESCs-OS expressed a wide range of osteoblast related genes including, runx2, Col 1A1, bone sialoprotein, and osteocalcin. Human ESCs-OS, hESCs-MSCs-OS, and hBMSCs-OS exhibited similar temporal gene expression patterns (Fig. 6). Human BMSCs demonstrated tendencies to express higher levels of osteoblast-associated genes than osteoblast-like cells derived from hESCs (hESCs-OS and hESCs-MSCs-OS). Significantly higher expression levels of hBMSCs than the other groups were found at each time point for most of the investigated genes (Fig. 6A, C, and D). The differences between hBMSCs and cells derived from hESCs were most noticeable for bone sialoprotein (Fig. 6C).

The pattern of ALP activity of hESCs-OS was comparable to hBMSCs-OS and hESCs-MSCs-OS except for the earliest cell culture period (Fig. 7A). Over time, levels of ALP activity of cells derived from hESCs gradually increased from basal levels, reaching the highest level on day 7 ($p< 0.05$), whereas

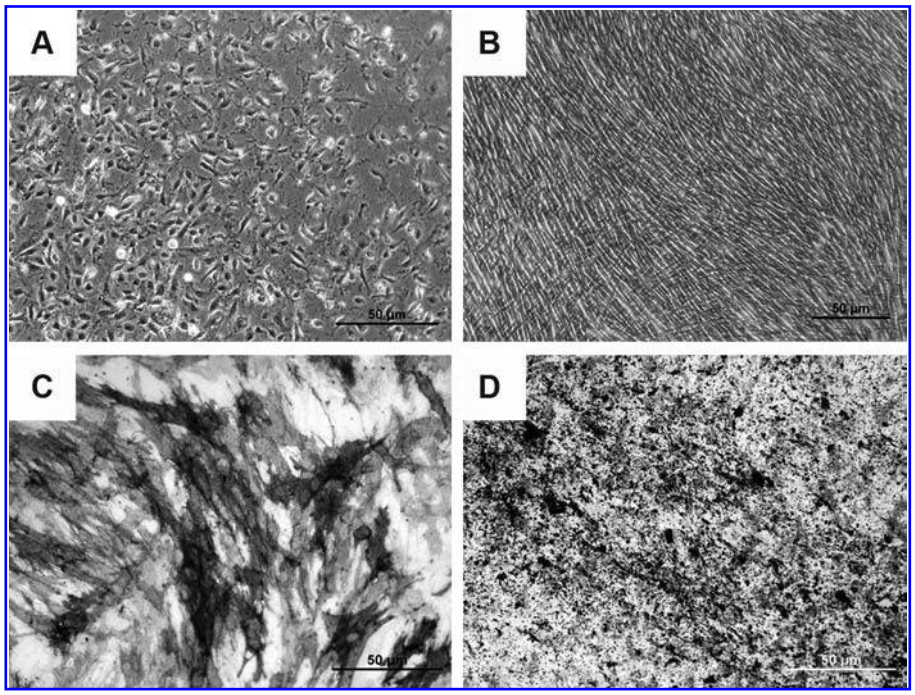

FIG. 3. Phase contrast images of hESC-derived osteoblast-like cells: (**A**) 7 days after initial cell seeding; (**B**) after the fifth passage on culture-day 21. (**C**) ALP staining at the fifth passage on day 14. (**D**) von Kossa staining of mineralized ECM at the fifth passage on day 21.

for hBMSCs-OS, the levels were constantly high from day 3 to day 7 ($p>0.05$). In all cell types the levels of ALP decreased to near basal levels by the end of the culture period. ALP activity of hBMSCs-OS on day 3 was significantly higher than that of hESCs-OS and hESCs-MSCs-OS ($p< 0.01$) (Fig. 7A).

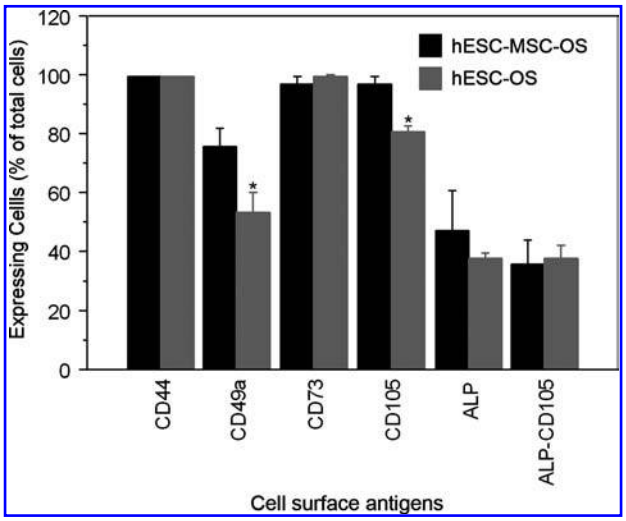

FIG. 4. Identification of mesenchymal stem cell (MSC) and osteoblast-associated surface antigens expressed by hESCs-MSCs (hESC-MSC-OS) and hESCs (hESC-OS, at passage 5) in osteogenic medium [CD44, CD49a, CD73, CD105, ALP, and double expression of ALP and CD105 (ALP-CD105)]. Results are presented as mean ± SEM of four independent experiments. The symbol (*) represents significantly higher levels relative to hESCs-OS ($p < 0.01$).

Osteocalcin levels in all groups, hESCs-OS, hESCs-MSCs-OS, and hBMSCs-OS were consistently low during the early cell culture period on days 7 and 14, and then significantly increased from day 14 to reach their highest levels on day 21 ($p <0.05$). Osteoclacin secretion levels from hESCs-OS were lower than hBMSCs-OS on day 7 and lower than both hBMSCs-OS and hESCs-MSCs-OS on day 14 ($p< 0.05$). However, on day 21, the expression levels of all groups were not significantly different ($p >0.05$) (Fig. 7B).

The differentiated hESC karyotypes were normal when tested at passages 5 and 10. All 20 G-banded metaphase cells demonstrated the normal 46XY karyotype (data not shown).

3D collagen scaffolds supported osteogenic differentiation of hESC-derived osteoblast-like cells

On culture-day 21, hESCs-OS differentiated into mature osteoblasts within the porous collagen scaffolds in osteogenic medium. Immunohistochemical staining of cell-scaffold constructs demonstrated the presence of ALP, collagen type I, osteonectin, and osteocalcin (Fig. 8A–E), whereas von Kossa staining identified mineralization of the ECM within the scaffold, where cells grew densely and formed a multilayer cell lining (Fig. 8F).

Human ESC-derived osteoblast-like cells formed bone in calvarial defects

To determine the bone forming capacity of the hESC-derived osteoblast-like cells, hESCs-OS at passages 5 and 10 were transplanted into critical size calvarial defects in immunodeficient mice. After 6 weeks, gross examination revealed irregular opacity in the area covering the defect site. Micro-CT images demonstrated limited amounts of new

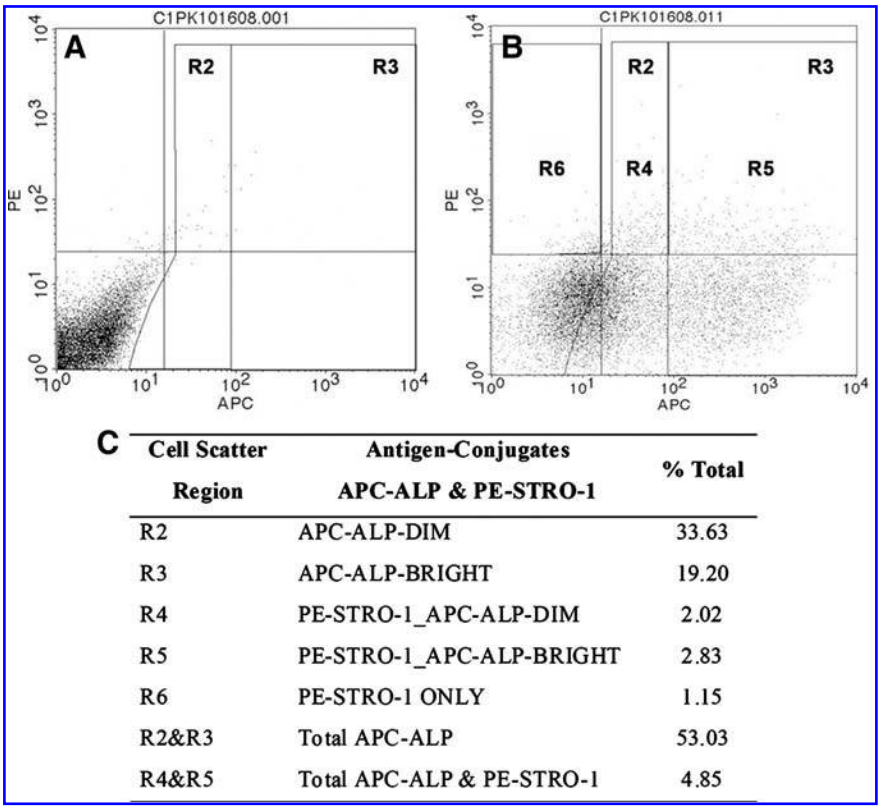

C

Cell Scatter Region	Antigen-Conjugates APC-ALP & PE-STRO-1	% Total
R2	APC-ALP-DIM	33.63
R3	APC-ALP-BRIGHT	19.20
R4	PE-STRO-1_APC-ALP-DIM	2.02
R5	PE-STRO-1_APC-ALP-BRIGHT	2.83
R6	PE-STRO-1 ONLY	1.15
R2&R3	Total APC-ALP	53.03
R4&R5	Total APC-ALP & PE-STRO-1	4.85

FIG. 5. Representative flow cytometry data set demonstrating expression profiles of the osteoblast-like cell surface antigens, alkaline phosphatase (ALP), and STRO-1, from hESC derived osteoblast-like cells (hESCs-OS) at passage 9. Side scatter analysis demonstrates: (**A**) negative control. (**B**) Double labeling of antibodies against APC-ALP (R2 and R3) and PE-STRO-1 conjugates (R4, R5, and R6). Gates R4 and R5 represent double expression of ALP-APC and STRO-1-PE and Gate R6 for expression of STRO-1-PE only. (**C**) Expression levels of APC-ALP (R2 and R3), PE-STRO-1_APC-ALP double staining (R4 and R5) and PE-STRO-1 only (R6). Results were derived from two different cell strains at passage 9. APC and PE represent allophycocyanin and phycoerythrin conjugates, respectively.

mineralized tissue within the central region, on the margin of the defect, and on the calvarial bone adjacent to the defect site. The new bone overlapping the native bone was likely caused by displacement of cell–fibrin gel-gelatin sponge constructs from the defect sites (Fig. 9A–C). Micro-CT analysis revealed that the BMD of new bone in the cranial defect generated by the transplanted cells at passage 5 was significantly higher than that of the controls without cells (BMD: 108.68±64.74mg HA/ccm vs. 35.258±3.0mg HA/ccm (Fig. 9E). When they were normalized to the controls, the BMD fold change of the samples to control was 3.11±1.85 ($p< 0.05$).

Histological evaluation confirmed incomplete healing of the defects; however, new bone was identified throughout the cranial defect. In the nonbone-forming area, the defect was filled with fibrous tissue and residual gelatin scaffold material (Fig. 9F and G). New bone formation appeared as woven or immature, as indicated by an unorganized bone matrix (Fig. 9H, I, and L) lined with numerous cuboidal-shaped osteoblast-like cells on the surface of newly formed bone (Fig. 9L). Hematopoietic bone marrow formation was found within the unorganized matrix of some bone nodules (Fig. 9H and I). Teratoma formation was not identified in any specimens at 6 weeks postimplantation.

Identification of human cells in the newly formed bone indicated an active role of transplanted cells in bone regeneration

Human cells were identified in the matrices of newly formed bone in both groups of transplanted cells at passages 5 and 10. Intense, bright red and dark brown nuclear staining of human specific nuclear antigen (HuNu) was localized in osteocytes and osteoblasts of newly formed bone (Fig. 9J and M). Nonspecific cytoplasmic staining of the surrounding connective tissue was sometimes observed. The specificity of the staining was supported by a negative control in which the primary antibody was omitted (Fig. 9K and N).

Discussion

The goal of this study was to generate large numbers of osteoblasts from hESCs by omitting the EB formation step, and to report an alternative method for generating osteogenic cells. An osteoblast differentiation protocol was developed to direct the differentiation of hESCs into the osteoblastic lineage and simultaneously expand the number of osteoblast-like cells. The findings suggest that large numbers of homogenous osteoblast-like cells can be derived from

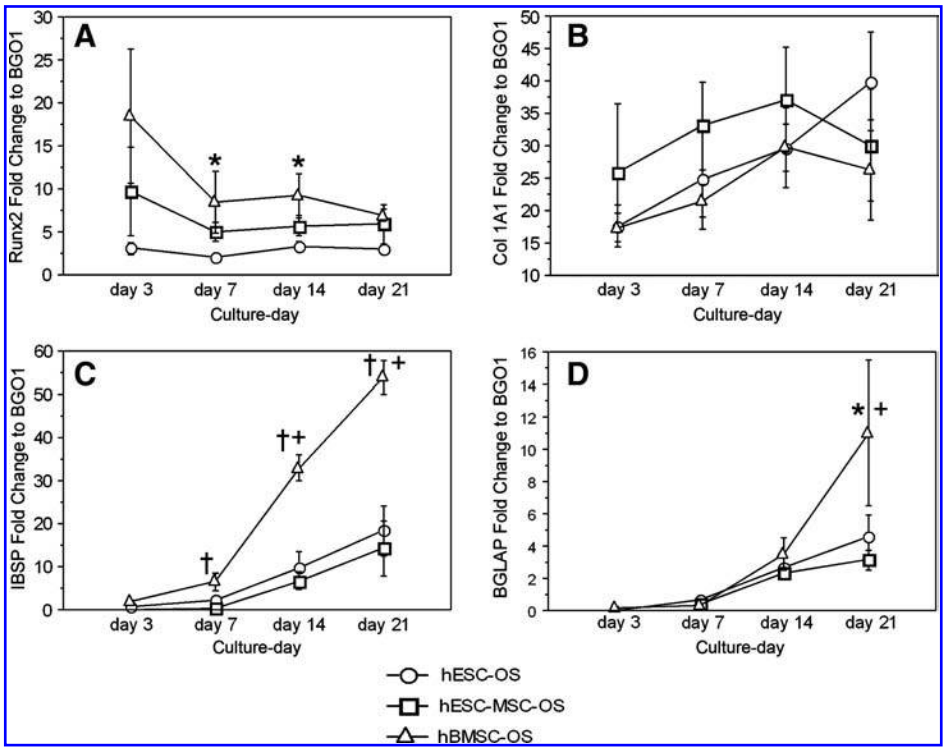

FIG. 6. Quantitative RT-PCR analysis of the expression profiles of osteoblast-associated genes, (**A**) Runx2, (**B**) Collagen type I (Col IA1), (**C**) bone sialoprotein (IBSP), and (**D**) Osteocalcin (BGLAP) from hESCs (hESC-OS), hESCs-MSCs (hESC-MSC-OS) and hBMSCs (hBMSC-OS) in osteogenic medium for a 21-day cell culture period. Results are presented as the mean ± SEM of three independent experiments normalized to the expression levels of undifferentiated hESCs (BGO1). The symbol (*) represents a significantly higher level relative to the group presenting the lowest level, (†) represents significantly higher levels relative to the other groups and (+) represents the significantly higher or lower levels relative to the values at different time points immediately before or after the indicated time ($p < 0.05$).

this protocol in a shorter period of time than the osteogenic induction of hESCs-MSCs (Arpornmaeklong et al., 2009).

It has been reported that undifferentiated cells persist when hESCs are differentiated in osteogenic medium at the primary passage (Figs. 1 and 2) (Karner et al., 2009; Sottile et al., 2003). The current study demonstrates a cell culture method to eliminate undifferentiated cells and generate a homogenous population of osteoblast-like cells from hESCs. This is achieved by consecutively expanding osteoprogenitor cells derived from hESCs in osteogenic medium through serial passaging (Fig. 1). The current cell culture model highlights advantages of serial passaging differentiated hESCs in osteogenic medium by eliminating undifferentiated cells, restricting the differentiation into the osteogenic lineage, and by increasing the numbers of osteoblast-like cells (Figs. 1, 2, and 6) (Arpornmaeklong et al., 2009; Banfi et al., 2000; Mendes et al., 2004). The expression of T-brachyury and osteoblast-related genes in hESCs-OS in the primary passage (Figs. 1 and 2) supports previous reports that hESCs can directly respond to osteogenic medium and transiently differentiate into cells of the mesodermal, mesenchymal, and osteoblastic lineages without first going through an EB stage (Arpornmaeklong et al., 2009; Karner et al., 2007; Karp et al., 2006).

The observation that hESCs-OS and hESCs-MSCs-OS expressed high levels of MSC surface antigens such as CD44, CD49a, CD73, and CD105 (Javazon et al., 2004) (Fig. 4), is consistent with our observation in a previous report on hESCs-MSCs-OS (Arpornmaeklong et al., 2009) and other reports on osteoblasts in different stages of differentiation (Arpornmaeklong et al., 2009; Bruder et al., 1998b; Chen et al., 1999; Jamal and Aubin, 1996; Zhou et al., 2008). This suggests that hESCs-OS may transition through a mesenchymal stem cell stage prior to differentiating to osteoblast-like cells.

The expression of osteoblast-related genes in hESCs at primary passage (Fig. 1) suggests that hESCs are able to spontaneously differentiate into osteoblast-like cells in culture medium without osteogenic supplementation and that osteogenic medium enhances osteoblastic differentiation (Karp et al., 2006). Likewise, the generation of osteoblast-like cells from either direct osteoblast induction of hESCs, or through an EB stage intermediary, both demonstrate an increase in expression of osteoblast-related genes over time in osteogenic medium (Bielby et al., 2004; Karner et al., 2007, 2009; Karp et al., 2006; Sottile et al., 2003) (Figs. 1 and 6). This supports the postulation that the serial passaging of differentiated cells in osteogenic medium would allow the expansion of a pool of osteoprogenitor cells to generate an enriched population of osteoblast-like cells (Bielby et al., 2004).

The differentiation of hESCs-OS into osteoblast-like cells in the late proliferative and matrix maturation stages was demonstrated by their expression of osteoblast-associated genes and osteoblastic phenotypes (Figs. 6 and 7) (Aubin, 1998; Jaiswal et al., 1997; Lynch et al., 1995). The FCM analysis, which showed low numbers of cells coexpressing

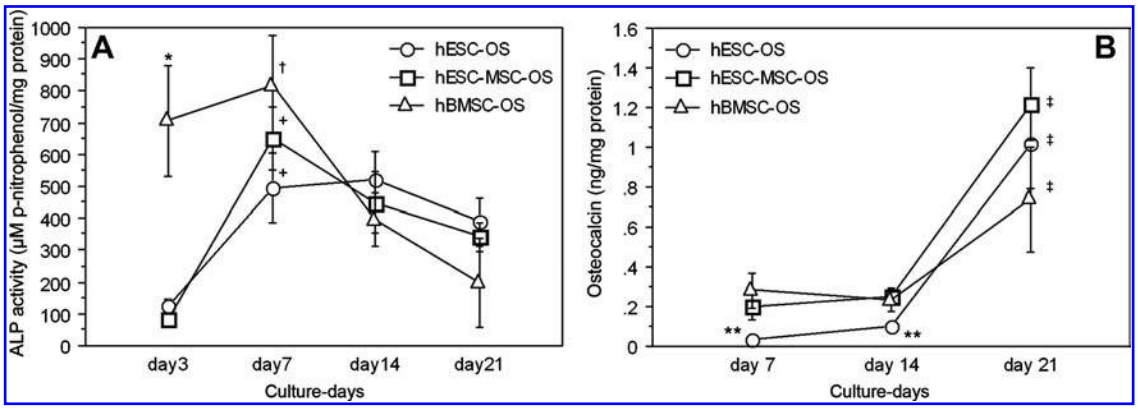

FIG. 7. Profiles of alkaline phosphatase (ALP) activity and osteocalcin secretion from hESCs (hESC-OS), hESCs-MSCs (hESC-MSC-OS), and hBMSCs (hBMSC-OS) in osteogenic medium during a 21-day cell culture period. (**A**) Levels of ALP activity on the cell membrane and extracellular matrix (ECM). (**B**) Levels of osteocalcin secretion in culture medium. Results are presented as the mean ± SEM of three independent experiments normalized to the total protein concentrations. The symbol (*) represents significantly higher ALP levels of hBMSCs-OS relative to hESCs-OS and hESCs-MSCs-OS ($p < 0.01$), (†) represents significantly higher ALP levels of hBMSCs-OS from day 7 to days 14 and 21 ($p < 0.05$), (+) represents the significantly higher ALP level of hESCs-OS and hESCs-MSCs-OS on day 7 to the levels on days 3, 14, and 21 ($p < 0.05$), (**) represents significantly lower osteocalcin levels of hESCs-OS relative to hBMSCs-OS on day 7 and to hBMSCs-OS and hESCs-MSCs-OS on day 14 ($p < 0.05$), and (‡) represents significantly higher levels of all three groups on day 21 relative to day 14 ($p < 0.05$).

STRO-1 and ALP (4%) and high numbers of ALP-expressing cells (40–50%) in hESCs-OS (Figs. 4 and 5) further demonstrates the differentiation of hESCs into osteoblast-like cells in the matrix maturation stage of differentiation *in vitro* (Gronthos et al., 1999). In addition to gene and phenotype expression profiles and the homogenous morphology of the cells (Figs. 3, 6, and 7), the absence of pluripotent gene expression and the lack of differentiation markers for cells of other lineages (Fig. 2), suggest that the hESCs-OS consist of an enriched population of osteoblast-like cells. Therefore, the current cell culture protocol facilitates the generation of committed osteoprogenitor cells that may be used for tissue regeneration and may reduce the risk of teratoma formation.

By directly introducing hESCs into osteogenic medium, we were able to generate large numbers of osteoblast-like cells (hESCs-OS) in a shorter period of time than the osteogenic induction through hESCs-MSCs. It was determined that as early as passage 5, the hESCs-OS expressed a full

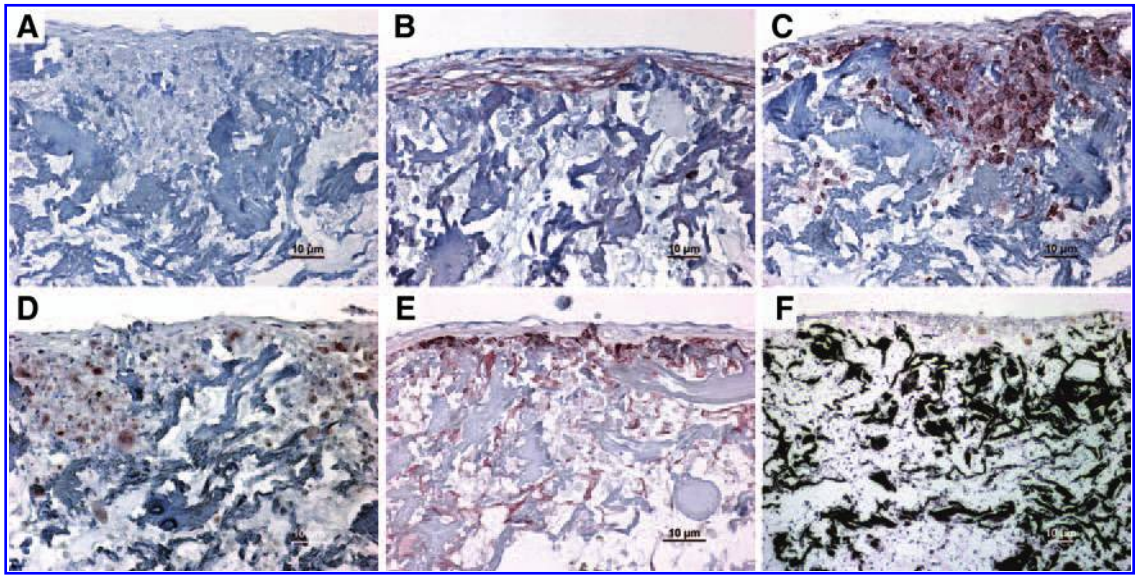

FIG 8. Human embryonic stem cell derived osteoblast-like cells (hESCs-OS) at passage 9 demonstrate an osteoblast-like phenotype in 3D scaffolds *in vitro*. The hESC-OS deposited and mineralized bone matrix proteins on porous collagen scaffolds during the 21-day culture. (**A–E**) Immunohistochemical staining of bone matrix proteins. (**A**) Negative control with omission of primary antibodies. (**B**) Antibodies against Collagen type I, (C) ALP, (**D**) Osteonectin, and (**E**) Osteocalcin. (**F**) von Kossa staining of mineralized matrices (black stain). The antigen-antibody complexes were detected by AEC substrate yielding a red-brown stain (**B–E**).

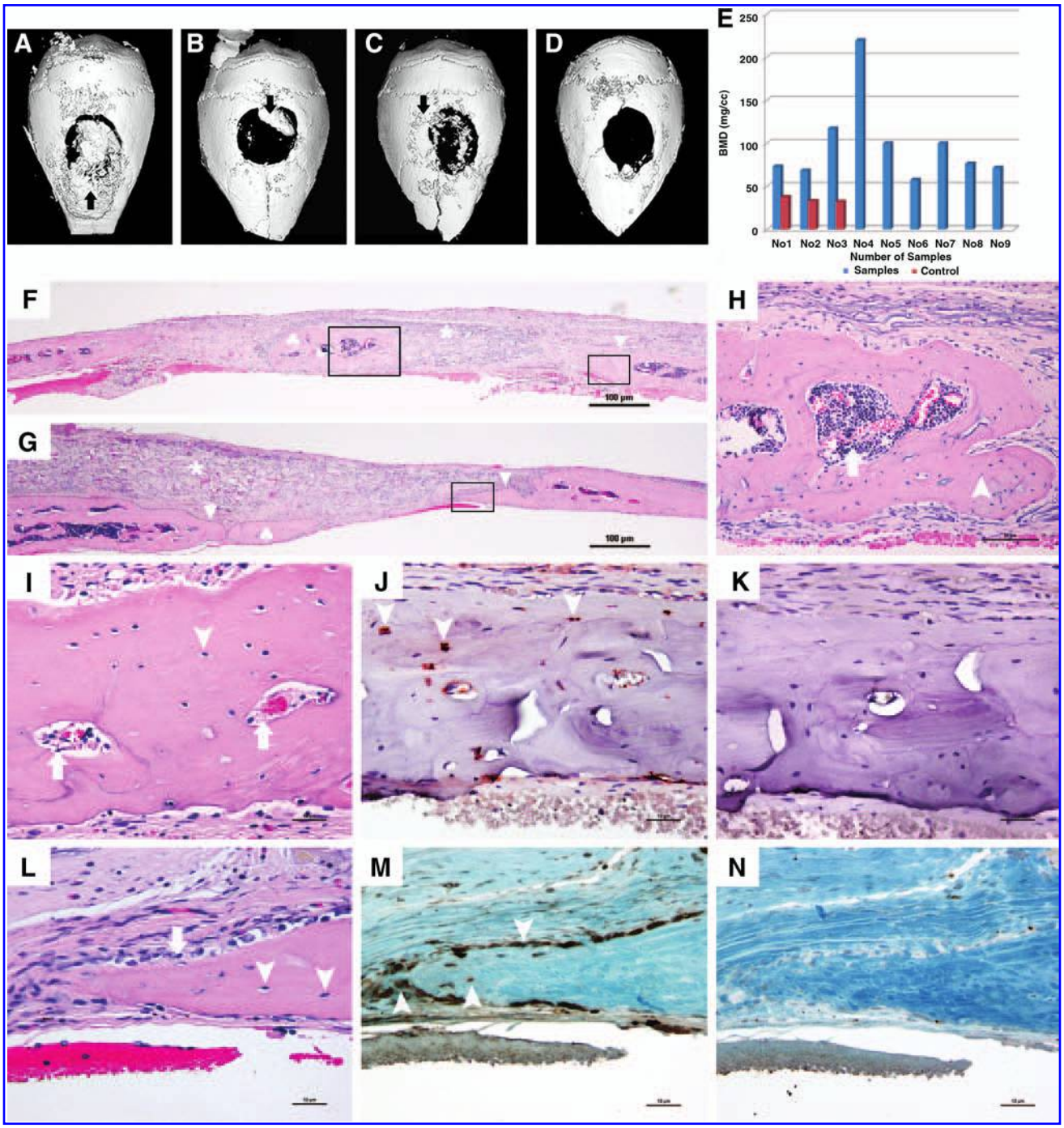

FIG. 9. Radiographic and histologic evaluation of hESCs-OS transplanted into calvarial defects at passages 5 and 10. Cells of human origin were identified in the newly formed bone. Representative three dimensional μCT images of hESCs-OS at passage 5 (A–C) demonstrate mineralized tissue formation in the central region, on the margin of the defect and on the calvarial bone adjacent to the defect site (arrows) and (**D**) the critical size defect in the control mouse with no transplanted cells. (**E**) Distribution of bone mineral density (BMD, mg HA/ccm) of newly formed bone from hESCs-OS at passage 5 in 10 experimental (blue columns) and 3 control mice (red columns). (**F, G**) Hematoxylin and eosin staining (H&E) of paraffin embedded sections of hESCs-OS at passage 5 (**F**) and at passage 10 (**G**), representing islands of newly formed bone in the central region (♣) and on the margin (▲) of the defects and the residual gelatin sponges (*). The boxed areas indicate selected regions of interest (ROI). (**H, I**) The magnified images from the selected ROI from (**F**) illustrate osteocytes embedded in unorganized matrix (arrow heads) and bone marrow (arrows). (**L**) Active bone formation is demonstrated by numerous osteoblast-like cells lining the surface of osteoid matrix (arrows) and osteocytes embedded in woven bone matrix (arrow heads). (**J**) Red nuclear staining of human specific nuclear antigen (HuNu) in osteocytes (arrow heads), derived from transplanted hESCs-OS at passage 5 were localized in the matrix of the newly formed bone on the margin of the defect defined by the small selected ROI in image F. (**M**) Brown nuclear staining of HuNu were localized in osteocytes (arrow heads) and osteoblast-like cells, derived from transplanted hESCs-OS at passage 10, lining the unorganized bone matrix (arrow) on the margin of the defect defined by the selected ROI in image G. (**K, N**) Negative controls with omission of a primary antibody.

range of osteoblast-associated genes and phenotypes in comparable patterns to hESCs-MSCs-OS and hBMSCs-OS (Figs. 6 and 7), and primary osteoblasts reported in previous studies (Aubin et al., 1995; Gronthos et al., 1999; Jaiswal et al., 1997). However, hESCs-MSCs-OS required a longer time in cell culture to reach this level of differentiation. This is because the hESCs were required to be in cell culture for six to seven passages to generate a homogenous population of MSCs before osteogenic differentiation of MSCs could be induced (Arpornmaeklong et al., 2009). Furthermore, it was observed that hESCs-OS and hESCs-MSCs-OS exhibited tendencies to express lower levels of osteoblast-associated genes than hBMSCs-OS. In particular, lower expression levels were observed for the transcription factor runx2 and bone sialoprotein, a late marker of osteogenic differentiation (Fig. 6) (Banfi et al., 2000; Jaiswal et al., 1997).

To apply differentiated hESCs in clinically relevant scenarios, a large number of cells are likely to be required. Likewise, the differentiation pattern and stability of osteoblastic differentiation during *in vitro* expansion and *in vivo* transplantation needs to be thoroughly characterized (Banfi et al., 2000; Miura et al., 2006). The ability to synthesize and mineralize bone matrices on 3D collagen scaffolds, and to form bone in the calvarial defect without teratoma formation (Figs. 8 and 9) demonstrated the phenotypic stability of hESCs-OS (Fenno et al., 2008; Kim et al., 2008; Tremoleda et al., 2008) and highlighted the similarity between hESCs-OS and osteoblast-like cells (Casser-Bette et al., 1990; Lynch et al., 1995). Therefore, the current findings demonstrate that osteoblast-like cells derived directly from hESCs in osteogenic medium are functional osteoblast-like cells that may be applicable for bone regeneration.

Moreover, the detection of human cells in the newly formed bone matrix (Fig. 9J and M) confirmed the fate of transplanted human cells as the bone forming cells (Abdallah et al., 2008; Kim et al., 2008), and thus demonstrate the bone regenerating capacity of the hESCs-OS in the skeletal defects. However, the ability of the scaffold to support cell viability (Kruyt et al., 2003) and the osteogenic differentiation capability of the transplanted cells in the defect sites (Bruder et al., 1998a; Miura et al., 2006) might have contributed to the limited and variable of amount of bone formed in this study (Fig. 9A–E).

Taken together, the advantages of the current cell culture model over the previously reported methods includes being less time consuming and the ability to generate an enriched population of osteoblast-like cells. Under the current cell culture protocol, osteoblast-like cells derived from hESCs in osteogenic medium are readily expandable and able to function as bone forming cells in a similar manner to hESCs-MSCs-OS and BMSC-OS. Therefore, cells derived from this method could potentially serve as a good source of osteoblast-like cells for studying osteoblast differentiation and bone tissue engineering.

Acknowledgments

This work was supported by NIH/NIDR R01DE 016530 (to P.H.K.). The authors thank the University of Michigan Stem Cell Core for support, the University of Michigan Orthopedic research lab, and Mrs. Colleen Flanagan for their assistance with microcomputed tomography, and the University of Michigan School of Dentistry Histology and Molecular biology Cores for their help with histology and molecular analyses.

Author Disclosure Statement

The authors declare no conflict of interest in connection with the submission of the current manuscript.

References

Abdallah, B.M., Ditzel, N., and Kassem, M. (2008). Assessment of bone formation capacity using in vivo transplantation assays: procedure and tissue analysis. Methods Mol. Biol. 455, 89–100.

Ahn, S.E., Kim, S., Park, K.H., et al. (2006). Primary bone-derived cells induce osteogenic differentiation without exogenous factors in human embryonic stem cells. Biochem. Biophys. Res. Commun. 340, 403–408.

Arpornmaeklong, P., Brown, S.E., Wang, Z., et al. (2009). Phenotypic characterization, osteoblastic differentiation, and bone regeneration capacity of human embryonic stem cell-derived mesenchymal stem cells. Stem Cells Dev. 18, 955–968.

Aubin, J.E. (1998). Advances in the osteoblast lineage. Biochem. Cell Biol. 76, 899–910.

Aubin, J.E., Liu, F., Malaval, L., et al. (1995). Osteoblast and chondroblast differentiation. Bone 17, 77S–83S.

Banfi, A., Muraglia, A., Dozin, B., et al. (2000). Proliferation kinetics and differentiation potential of ex vivo expanded human bone marrow stromal cells: implications for their use in cell therapy. Exp. Hematol. 28, 707–715.

Barberi, T., Willis, L.M., Socci, N.D., et al. (2005). Derivation of multipotent mesenchymal precursors from human embryonic stem cells. PLoS Med. 2, e161.

Bianco, P., and Robey, P.G. (2001). Stem cells in tissue engineering. Nature 414, 118–121.

Bielby, R.C., Boccaccini, A.R., Polak, J.M., et al. (2004). In vitro differentiation and in vivo mineralization of osteogenic cells derived from human embryonic stem cells. Tissue Eng. 10, 1518–1525.

Brown, S.E., Tong, W., and Krebsbach, P.H. (2009). The derivation of mesenchymal stem cells from human embryonic stem cells. Cells Tissues Organs 189, 256–260.

Bruder, S.P., Jaiswal, N., Ricalton, N.S., et al. (1998a). Mesenchymal stem cells in osteobiology and applied bone regeneration. Clin. Orthop. Relat. Res. S247–S256.

Bruder, S.P., Ricalton, N.S., Boynton, R.E., et al. (1998b). Mesenchymal stem cell surface antigen SB-10 corresponds to activated leukocyte cell adhesion molecule and is involved in osteogenic differentiation. J. Bone Miner. Res. 13, 655–663.

Bunnell, B.A., Estes, B.T., Guilak, F., et al. (2008). Differentiation of adipose stem cells. Methods Mol. Biol. 456, 155–171.

Cancedda, R., Mastrogiacomo, M., Bianchi, G., et al. (2003). Bone marrow stromal cells and their use in regenerating bone. Novartis Found. Symp. 249, 133–143; discussion 143–137, 170–134, 239–241.

Cao, T., Heng, B.C., Ye, C.P., et al. (2005). Osteogenic differentiation within intact human embryoid bodies result in a marked increase in osteocalcin secretion after 12 days of in vitro culture, and formation of morphologically distinct nodule-like structures. Tissue Cell. 37, 325–334.

Carpenter, M.K., Rosler, E., and Rao, M.S. (2003). Characterization and differentiation of human embryonic stem cells. Cloning Stem Cells 5, 79–88.

Casser-Bette, M., Murray, A.B., Closs, E.I., et al. (1990). Bone formation by osteoblast-like cells in a three-dimensional cell culture. Calcif. Tissue Int. 46, 46–56.

Chen, X.D., Qian, H.Y., Neff, L., et al. (1999). Thy-1 antigen expression by cells in the osteoblast lineage. J. Bone Miner. Res. 14, 362–375.

Derubeis, A.R., and Cancedda, R. (2004). Bone marrow stromal cells (BMSCs) in bone engineering: limitations and recent advances. Ann Biomed Eng. 32, 160–165.

De Ugarte, D.A., Alfonso, Z., Zuk, P.A., et al. (2003). Differential expression of stem cell mobilization-associated molecules on multi-lineage cells from adipose tissue and bone marrow. Immunol. Lett. 89, 267–270.

Fenno, L.E., Ptaszek, L.M., and Cowan, C.A. (2008). Human embryonic stem cells: emerging technologies and practical applications. Curr. Opin. Genet. Dev. 18, 324–329.

Gronthos, S., Zannettino, A.C., Graves, S.E., et al. (1999). Differential cell surface expression of the STRO-1 and alkaline phosphatase antigens on discrete developmental stages in primary cultures of human bone cells. J. Bone Miner. Res. 14, 47–56.

Heng, B.C., Cao, T., Stanton, L.W., et al. (2004). Strategies for directing the differentiation of stem cells into the osteogenic lineage in vitro. J. Bone Miner. Res. 19, 1379–1394.

Hu, W.W., Wang, Z., Hollister, S.J., et al. (2007). Localized viral vector delivery to enhance in situ regenerative gene therapy. Gene Ther. 14, 891–901.

Jaiswal, N., Haynesworth, S.E., Caplan, A.I., et al. (1997). Osteogenic differentiation of purified, culture-expanded human mesenchymal stem cells in vitro. J. Cell Biochem. 64, 295–312.

Jamal, H.H., and Aubin, J.E. (1996). CD44 expression in fetal rat bone: in vivo and in vitro analysis. Exp. Cell Res. 223, 467–477.

Javazon, E.H., Beggs, K.J., and Flake, A.W. (2004). Mesenchymal stem cells: paradoxes of passaging. Exp. Hematol. 32, 414–425.

Karner, E., Backesjo, C.M., Cedervall, J., et al. (2009). Dynamics of gene expression during bone matrix formation in osteogenic cultures derived from human embryonic stem cells in vitro. Biochim. Biophys. Acta 1790, 110–118.

Karner, E., Unger, C., Sloan, A.J., et al. (2007). Bone matrix formation in osteogenic cultures derived from human embryonic stem cells in vitro. Stem Cells Dev. 16, 39–52.

Karp, J.M., Ferreira, L.S., Khademhosseini, A., et al. (2006). Cultivation of human embryonic stem cells without the embryoid body step enhances osteogenesis in vitro. Stem Cells 24, 835–843.

Kim, S., Kim, S.S., Lee, S.H., et al. (2008). In vivo bone formation from human embryonic stem cell-derived osteogenic cells in poly(d,l-lactic-co-glycolic acid)/hydroxyapatite composite scaffolds. Biomaterials. 29, 1043–1053.

Krebsbach, P.H., Kuznetsov, S.A., Satomura, K., et al. (1997). Bone formation in vivo: comparison of osteogenesis by transplanted mouse and human marrow stromal fibroblasts. Transplantation. 63, 1059–1069.

Krebsbach, P.H., Mankani, M.H., Satomura, K., et al. (1998). Repair of craniotomy defects using bone marrow stromal cells. Transplantation 66, 1272–1278.

Kruyt, M.C., de Bruijn, J.D., Wilson, C.E., et al. (2003). Viable osteogenic cells are obligatory for tissue-engineered ectopic bone formation in goats. Tissue Eng. 9, 327–336.

Kwan, M.D., Slater, B.J., Wan, D.C., et al. (2008). Cell-based therapies for skeletal regenerative medicine. Hum. Mol. Genet. 17, R93–R98.

Lannert, H., Able, T., Becker, S., et al. (2008). Optimizing BM harvesting from normal adult donors. Bone Marrow Transplant. 42, 443–447.

Lynch, M.P., Stein, J.L., Stein, G.S., et al. (1995). The influence of type I collagen on the development and maintenance of the osteoblast phenotype in primary and passaged rat calvarial osteoblasts: modification of expression of genes supporting cell growth, adhesion, and extracellular matrix mineralization. Exp. Cell Res. 216, 35–45.

Martin, I., Muraglia, A., Campanile, G., et al. (1997). Fibroblast growth factor-2 supports ex vivo expansion and maintenance of osteogenic precursors from human bone marrow. Endocrinology 138, 4456–4462.

Mendes, S.C., Tibbe, J.M., Veenhof, M., et al. (2004). Relation between in vitro and in vivo osteogenic potential of cultured human bone marrow stromal cells. J. Mater. Sci. Mater. Med. 15, 1123–1128.

Miura, M., Miura, Y., Sonoyama, W., et al. (2006). Bone marrow-derived mesenchymal stem cells for regenerative medicine in craniofacial region. Oral Dis. 12, 514–522.

Olivier, E.N., Rybicki, A.C., and Bouhassira, E.E. (2006). Differentiation of human embryonic stem cells into bipotent mesenchymal stem cells. Stem Cells 24, 1914–1922.

Pittenger, M.F., Mackay, A.M., Beck, S.C., et al. (1999). Multilineage potential of adult human mesenchymal stem cells. Science 284, 143–147.

Quarto, R., Thomas, D., and Liang, C.T. (1995). Bone progenitor cell deficits and the age-associated decline in bone repair capacity. Calcif. Tissue Int. 56, 123–129.

Sottile, V., Thomson, A., and McWhir, J. (2003). In vitro osteogenic differentiation of human ES cells. Cloning Stem Cells. 5, 149–155.

Tremoleda, J.L., Forsyth, N.R., Khan, N.S., et al. (2008). Bone tissue formation from human embryonic stem cells in vivo. Cloning Stem Cells 10, 119–132.

Trivedi, P., and Hematti, P. (2007). Simultaneous generation of CD34+ primitive hematopoietic cells and CD73+ mesenchymal stem cells from human embryonic stem cells cocultured with murine OP9 stromal cells. Exp. Hematol. 35, 146–154.

Zhou, Y., Hutmacher, D.W., Sae-Lim, V., et al. (2008). Osteogenic and adipogenic induction potential of human periodontal cells. J. Periodontol. 79, 525–534.

Address correspondence to:
Prof. Paul H. Krebsbach, D.D.S., Ph.D.
Department of Biologic and Materials Sciences
University of Michigan School of Dentistry
1011 North University Avenue, Rm 1030 Kellogg
Ann Arbor, MI 48109-1078

E-mail: paulk@umich.edu